J. Chem. Sci. Vol. 128, No. 8, August 2016, pp. 1337–1343. © Indian Academy of Sciences.
DOI 10.1007/s12039-016-1124-y

A fluorescent sensor based on binaphthol-quinoline Schiff base for relay recognition of Zn^{2+} and oxalate in aqueous media

LIJUN TANG*, DI WU, ZHENLONG HUANG and YANJIANG BIAN
Department of Chemistry, Bohai University, Jinzhou 121013, China
e-mail: ljtang@bhu.edu.cn

MS received 8 October 2015; revised 10 May 2016; accepted 27 May 2016

Abstract. To develop an effective fluorescent chemosensor for relay recognition of Zn^{2+} and oxalate, a new fluorescent sensor based on binaphthol-quinoline Schiff base $\mathbf{L_1}$ was designed and synthesized. In DMSO-H_2O (1/1, v/v, HEPES 10 mM, pH = 7.4) solution, $\mathbf{L_1}$ exhibits highly selective fluorescence turn on response to Zn^{2+} over other metal ions. The Zn^{2+} recognition event is barely interfered by other coexisting metal ions except Cu^{2+}, Co^{2+} and Ni^{2+}. The *in situ* generated $\mathbf{L_1}$-Zn^{2+}complex was further used as a chemosensing ensemble for oxalate detection. The complex $\mathbf{L_1}$-Zn^{2+} displays high selectivity to oxalate with significant fluorescence quenching through Zn^{2+} ion displacement approach. In addition, application of $\mathbf{L_1}$ for imaging of Zn^{2+} and oxalate in living HeLa cells was also examined.

Keywords. Zn^{2+} sensing; oxalate sensing; fluorescence; relay recognition

1. Introduction

The development of chemosensors for highly selective detection of biologically and environmentally important metal ions and anions has received increasing attention owing to the vital roles they play in chemical, biological and environmental processes.[1] Zn^{2+}, the second most abundant transition metal ion in human body, plays paramount roles in a wide range of biological processes such as gene transcription, signal transmission, and mammalian reproduction. Disruption of Zn^{2+} concentration in cells can result in a variety of pathological processes including Alzheimer's disease, epilepsy and infantile diarrhea.[2] Therefore, there is a growing interest in developing selective and sensitive Zn^{2+} sensors to recognize the physiological significance of Zn^{2+} and its biomedical relevance.[3]

Among the biologically pivotal anions, oxalate is particularly important due to its important role especially in food chemistry and clinical analysis. Although various methods including enzyme electrode assay,[4] chromatography,[5] electrophoresis and electrochemistry[6] have been used for oxalate detection, fluorescence recognition of oxalate has received substantial attention due to its simplicity and waiver of sophisticated sample pretreatment.[7] Recent use of single sensor for relay recognition of metal ion and anion has aroused considerable interest of researchers due to the operational simplicity.[8] As far as we are aware, utilization of a single sensor for relay recognition of Zn^{2+} and oxalate has not been documented.

Herein, a fluorescence sensor based on Schiff base $\mathbf{L_1}$ (Scheme 1) for sequential detection of Zn^{2+} and oxalate has been synthesized, which exhibits relay recognition behavior toward Zn^{2+} and oxalate in aqueous solution through fluorescence 'off-on-off' changes.

2. Experimental

2.1 *Instruments and reagents*

Unless otherwise stated, solvents and reagents were purchased as analytical grade and were used without further purification. Double distilled water was used for spectral detection. ^{1}H NMR and ^{13}C NMR spectra were performed on an Agilent 400 MR spectrometer, and the chemical shifts (δ) were expressed in ppm and coupling constants (J) in Hertz. High-resolution mass spectroscopy (HRMS) was conducted on a Bruker micrOTOF-Q mass spectrometer. Fluorescence measurements were carried out on a Sanco 970-CRT spectrofluorometer (Shanghai Spectrum instruments Co., Ltd., China). UV-vis absorption spectra were recorded on a SP-1900 spectrophotometer (Shanghai Spectrum instruments Co., Ltd., China). The pH measurements were made with a Model PHS-25B meter (Shanghai, China).

*For correspondence

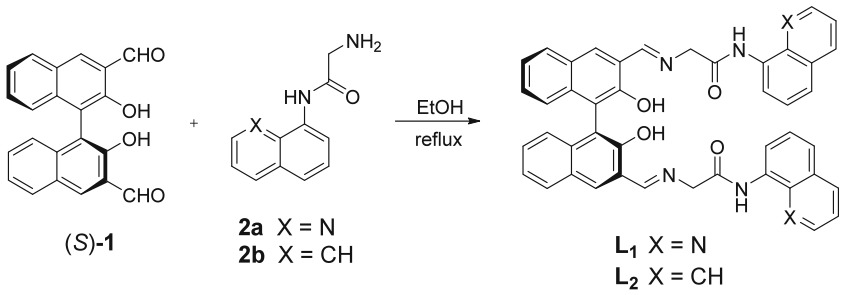

Scheme 1. Synthesis of sensor $\mathbf{L_1}$ and control compound $\mathbf{L_2}$.

2.2 *Synthesis of chemosensor L_1 and control compound L_2*

Chemosensor $\mathbf{L_1}$ was synthesized as follows. A stirred solution of compounds (*S*)-**1**[9] (342 mg, 1 mmol) and **2a**[10] (502.5 mg, 2.5 mmol) in absolute ethanol (50 mL) was heated to reflux for 2 h. After cooling to room temperature, the yellow precipitate formed was collected by filtration, which was washed three times with cold ethanol to give pure $\mathbf{L_1}$. Yield: 566 mg, 0.80%; M.p.: 207-208°C;. ^{1}H NMR (400 MHz, DMSO-d_6)δ: 12.70 (s, 2H, -OH), 10.58 (s, 2H, -NH), 9.01 (s, 2H, N=CH), 8.56 (d, J = 7.6 Hz, 2H, Ar-H), 8.49 (d, J = 3.2 Hz, 2H, Ar-H), 8.38 (s, 2H, Ar-H), 8.23 (d, J = 8.0 Hz, 2H, Ar-H), 8.07-8.05 (m, 2H, Ar-H), 7.59-7.50 (m, 5H, Ar-H), 7.43 (dd, J = 7.6, 4.0 Hz, 2H, Ar-H), 7.38-7.36 (m, 3H, Ar-H), 7.17-7.09 (m, 2H, Ar-H), 4.78 (dd, J = 16.4 Hz, 4H, -CH_2-); ^{13}C NMR (100 MHz, $CDCl_3$)δ: 168.89, 166.71, 154.33, 148.48, 138.21, 135.90, 135.38, 134.86, 133.47, 129.17, 128.87, 127.66, 127.37, 126.78, 124.92, 123.59, 121.90, 121.29, 120.79, 117.09, 115.91, 64.05; HRMS-ESI(+): m/z = 709.2550 $[M+1]^+$.

Control compound $\mathbf{L_2}$ was synthesized by a similar procedure was used for that of $\mathbf{L_1}$ except that **2b**[11] was used. Yield: 600 mg, 85%; M.p.: 159-160°C; ^{1}H NMR (400 MHz, DMSO-d_6)δ: 13.06 (s, 2H, -OH), 10.20 (s, 2H, NH), 8.96 (s, 2H, N=CH), 8.34 (s, 2H, Ar-H), 8.04 (t, J = 7.2 Hz, 4H, Ar-H), 7.91 (d, J = 7.6 Hz, 2H, Ar-H), 7.76 (d, J = 8.0 Hz, 2H, Ar-H), 7.68 (d, J = 7.2 Hz, 2H, Ar-H), 7.52-7.45 (m, 6H, Ar-H), 7.37-7.31 (m, 4H, Ar-H), 7.05 (d, J = 8.4 Hz, 2H, Ar-H), 4.72 (s, 4H, -CH_2-); ^{13}C NMR (100 MHz, DMSO-d_6)δ:169.70, 168.07, 154.80, 135.30, 134.22, 134.13, 133.58, 129.57, 128.83, 128.56, 128.27, 127.55, 126.50, 126.33, 125.99, 125.17, 124.63, 123.68, 123.12, 122.33, 121.28, 116.61, 62.31; HRMS-ESI(+): m/z = 707.2653 $[M+1]^+$.

For ^{1}H NMR spectra of $\mathbf{L_1}$ and $\mathbf{L_2}$, please see Figures S1 and S2 (in Supplementary Information).

3. Results and Discussion

3.1 *Fluorescence recognition of Zn^{2+} by L_1*

Chemosensor $\mathbf{L_1}$ was synthesized by condensation of (*S*)-**1** and **2a** in absolute ethanol, and the structure of $\mathbf{L_1}$ was fully characterized by ^{1}H NMR, ^{13}C NMR and HRMS analysis. The fluorescence responses of $\mathbf{L_1}$ (10 μM) to various metal ions were investigated in DMSO-H_2O (1/1, v/v, HEPES 10 mM, pH = 7.4) solution (Figure 1). $\mathbf{L_1}$ itself displays almost negligible fluorescence emission on excitation at 359 nm, which may attributed to the combined effects of PET from phenolic moiety to quinoline fluorophore and the isomerization process of C=N bond.[12] Upon addition of 4.0 equiv. of Zn^{2+}, a dramatic fluorescence enhancement at 512nm was observed, which could be attributed to the Zn^{2+} -binding induced suppression of PET and C=N isome rization. The Zn^{2+} induced green fluorescence color of

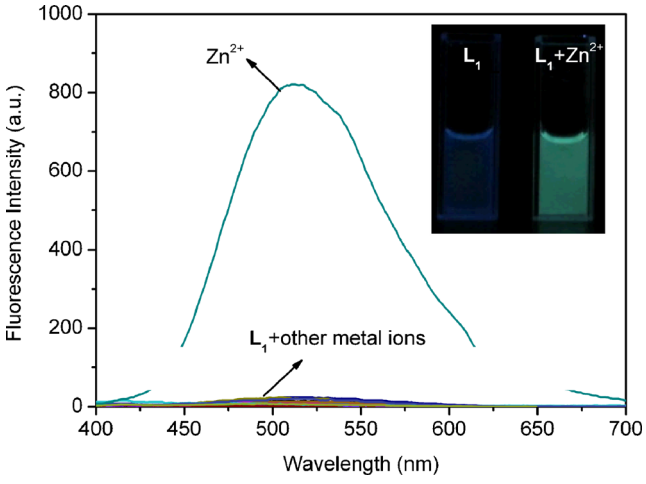

Figure 1. Changes in the fluorescence emission of $\mathbf{L_1}$ (10 μM) in DMSO-H_2O (1/1, v/v, HEPES 10 mM, pH = 7.4) solution upon addition of 4 equiv. of various metal ion. Inset: naked eye observed fluorescence changes of $\mathbf{L_1}$ solution in the presence of Zn^{2+} ions under a portable UV lamp at 365 nm.

L_1 solution can be observed by a naked eye under illumination at 365 nm with a portable UV lamp (Figure 1, inset). Whereas, addition of equal amounts of other metal ions such as K^+, Na^+, Ag^+, Pb^{2+}, Sr^{2+}, Ba^{2+}, Cd^{2+}, Fe^{2+}, Fe^{3+}, Mn^{2+}, Mg^{2+}, Cr^{3+}, Al^{3+}, Ni^+, Co^{2+}, Ca^{2+}, Cu^{2+} and Hg^{2+}, promoted negligible fluorescence intensity changes of **L_1**. The observed emission at 512 nm was supposed to come from the quinoline fluorophore,[13] and this hypothesis was confirmed by comparison of fluorescence responses of control compound **L_2** and sensor **L_1** to Zn^{2+} ion (Figure S3). Under identical conditions, **L_2** does not show any noticeable fluorescence emission in the absence and presence of Zn^{2+}, indicating that the quinoline moiety is responsible for the observed "turn-on" fluorescence of **L_1**. These results indicate that **L_1** has an excellent selectivity toward Zn^{2+} ion.

The Zn^{2+} sensing behavior of **L_1** to Zn^{2+} was then explored by fluorescence titration experiments. Incremental addition of Zn^{2+} to **L_1** solution led to gradual increase in fluorescence intensity at 512 nm, which reached a plateau when 4.0 equiv. of Zn^{2+} was employed (Figure 2). Plotting of the normalized fluorescence intensity $((I\text{-}I_{min})/(I_{max}\text{-}I_{min}))$ at 512 nm against Log[Zn^{2+}] results in a neat linear relation (R = 0.9977) (Figure 3), and the detection limit of **L_1** to Zn^{2+} was calculated to be 1.5×10^{-6} M.[14] The association constant (K_s) of **L_1** and Zn^{2+} was estimated to be 2.15×10^6 M^{-1} by non-linear least squares fitting of the titration data based on a 1:1 binding equation model (Figure 4). In addition, this 1:1 binding ratio was also supported by Job's plot analysis (Figure S4). The UV-vis absorption spectrum of **L_1** on incremental addition of Zn^{2+} shows ratiometric absorption changes (Figure S5). The absorption band at 394 nm of **L_1** can be assigned to the absorption of Schiff base linked binol moiety. On gradual addition of Zn^{2+} to **L_1** solution, the absorption intensity of **L_1** at 394 nm decreased gradually, concomitantly, two new absorption bands centered at 357 nm and 443 nm emerged and gradually increased, and they can be attributed to the deprotonated amide-quinoline[13] and phenolic binol Schiff base,[15] respectively.

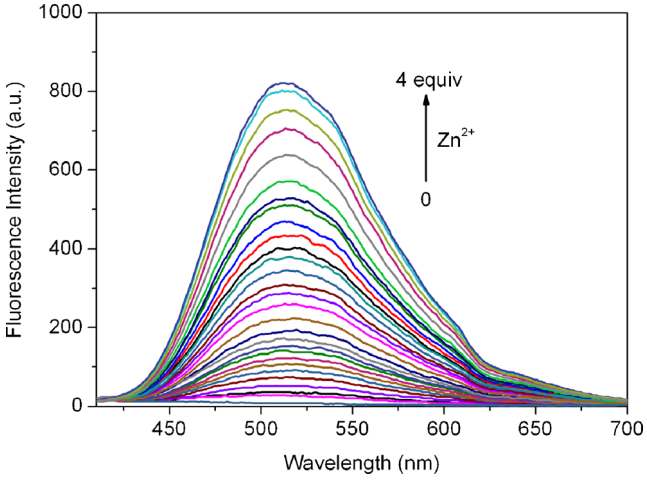

Figure 2. Fluorescence spectra changes of sensor **L_1** (10 μM) in DMSO-H_2O (1/1, v/v, HEPES 10 mM, pH = 7.4) solution on step increasing in Zn^{2+} concentration (0 to 40 μM).

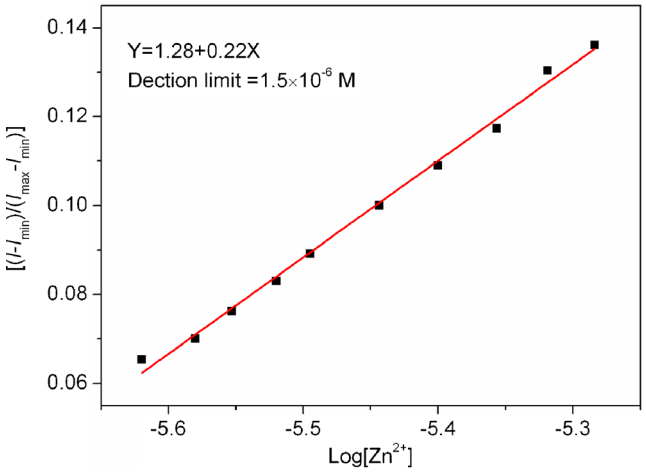

Figure 3. Normalized fluorescence intensity of **L_1** solution (10 μM) to Log[Zn^{2+}]; unit for [Zn^{2+}] is M.

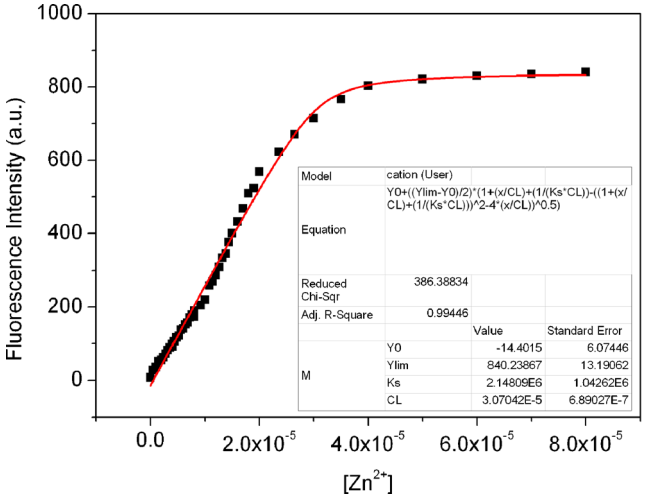

Figure 4. Nonlinear least-squares fitting of fluorescence intensity of **L_1**(at 512 nm) employing a 1:1 binding mode equation. Unit for [Zn^{2+}] is M.

To corroborate the high selectivity of **L_1** to Zn^{2+}, the competition experiments were subsequently carried out. As shown in Figure 5, on further addition of 4.0 equiv. of Zn^{2+} to the competitive metal ion containing **L_1** solution, a dramatic fluorescence emission enhancement was observed except for Cu^{2+}, Ni^{2+} and Co^{2+}. The influence of Cu^{2+} is owing to its paramagnetic nature. On the other hand, the level of Ni^{2+} and Co^{2+} are very low in human body and they will have little influences on Zn^{2+} recognition in living cells. These

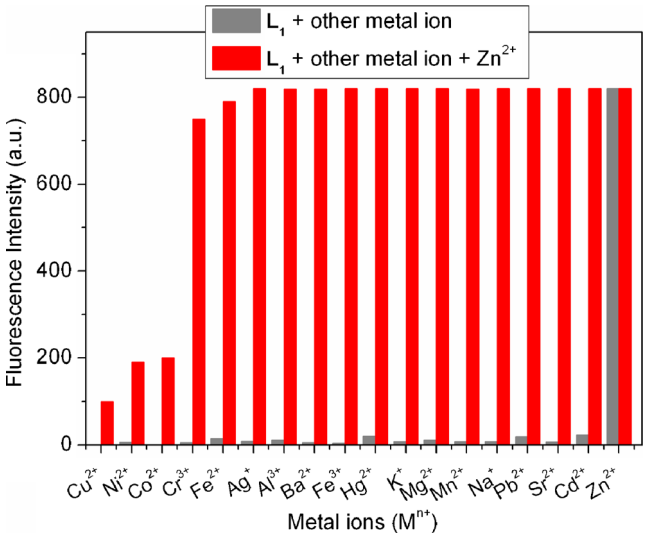

Figure 5. Fluorescence intensity of $\mathbf{L_1}$ (10 μM) in H_2O-DMSO (1/1, v/v, pH = 7.4) at 512 nm. The gray bars represent the emission intensity of $\mathbf{L_1}$ in the presence of 4.0 equiv. of competing metal ion; the red bars represent the emission intensity of the above solution upon addition of 4.0 equiv. of Zn^{2+}.

results reveal that $\mathbf{L_1}$ still has a potential applicability for Zn^{2+} detection.

To obtain further insight into the binding mode of $\mathbf{L_1}$ with Zn^{2+}, ^{1}H NMR spectra of $\mathbf{L_1}$ in the absence and presence of Zn^{2+} were compared (Figure 6). The broad peak at 12.70 ppm in free $\mathbf{L_1}$ is assigned to the hydroxyl proton (H_a) (Figure 6a), which is greatly decreased upon addition of 2.0 equiv. of Zn^{2+} (Figure 6b), indicating the Zn^{2+} binding induced de-protonation process. The imine protons (H_b) in $\mathbf{L_1}$ at 9.01 ppm (Figure 6a) shifted downfield to 10.76 ppm on interaction with Zn^{2+} (Figure 6b). The amide proton signal (H_d) in $\mathbf{L_1}$ at 10.58 ppm (Figure 6a) was greatly decreased on addition of Zn^{2+} (Figure 6b), indicative of the deprotonation of amide group. Moreover, the quinolone proton signals of H_e (8.49 ppm) and H_j (8.56 ppm) in free $\mathbf{L_1}$ also shifted downfield to 8.98 ppm and 8.64 ppm, respectively. These results reveal that the phenolic oxygen, imine and amide nitrogen, and quinolone nitrogen atoms are all involved in the complex formation. Thus, a plausible binding mode of $\mathbf{L_1}$ with Zn^{2+} ions was proposed and is illustrated in Scheme 2.

3.2 *Fluorescence recognition of oxalate by $\mathbf{L_1}$-Zn^{2+} complex*

The *in situ* formed $\mathbf{L_1}$-Zn^{2+} complex (prepared by mixing $\mathbf{L_1}$ with 4.0 equiv. of Zn^{2+}) was envisioned to be a potential candidate for chemosensing ensemble of dicarboxylate recognition. Upon individual addition of 100 equiv. (relative to $\mathbf{L_1}$) of different dicarboxylates to $\mathbf{L_1}$-Zn^{2+} solution (10 μM based on $\mathbf{L_1}$), oxalate elicited a dramatic fluorescence quenching, which is similar to the original emission state of free $\mathbf{L_1}$ (Figure 7). Considering the low solubility of ZnC_2O_4 ($K_{sp} = 2.8\times10^{-8}$), the observed fluorescence quenching is due to oxalate-induced de-complexation of $\mathbf{L_1}$-Zn^{2+} complex. Nevertheless, addition of other dicarboxylates including succinate, glutarate, adipate, phthalate, terephthalate, and isophthalate caused no significant fluorescence spectrum changes except that malonate promoted a slight decrease in fluorescence emission. These results demonstrate that the *in situ* generated $\mathbf{L_1}$-Zn^{2+} complex can act as an ensemble for oxalate recognition. Fluorescence titration with oxalate results in gradual emission quenching of Zn^{2+}-$\mathbf{L_1}$ at 512 nm, and the quenching process terminated when 100 equiv. of oxalate was added (Figure 8). Based on the titration data, the

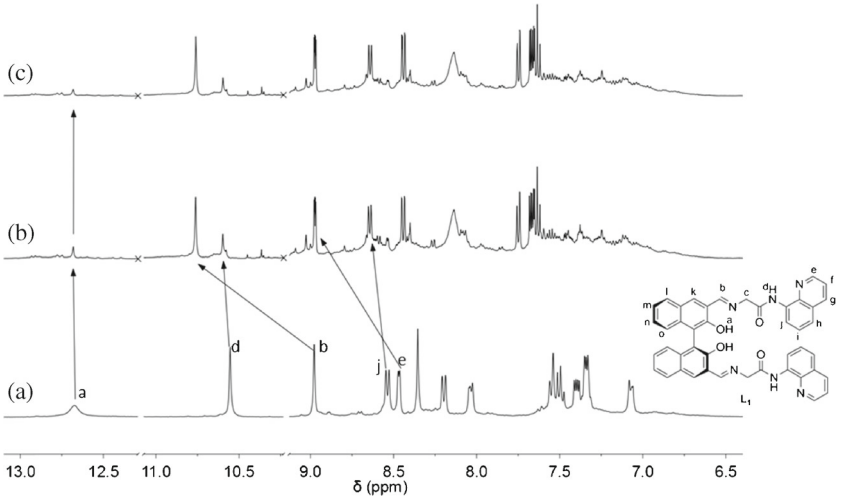

Figure 6. Partial ^{1}H NMR spectrum (in DMSO-d_6) of $\mathbf{L_1}$ in the presence of 0 (a), 2.0 (b) and 2.5 (c) equivalents of Zn^{2+}.

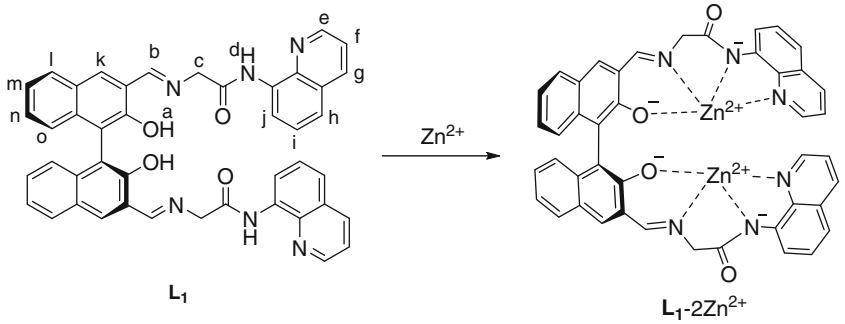

Scheme 2. Proposed binding mode between $\mathbf{L_1}$ and Zn^{2+} ions.

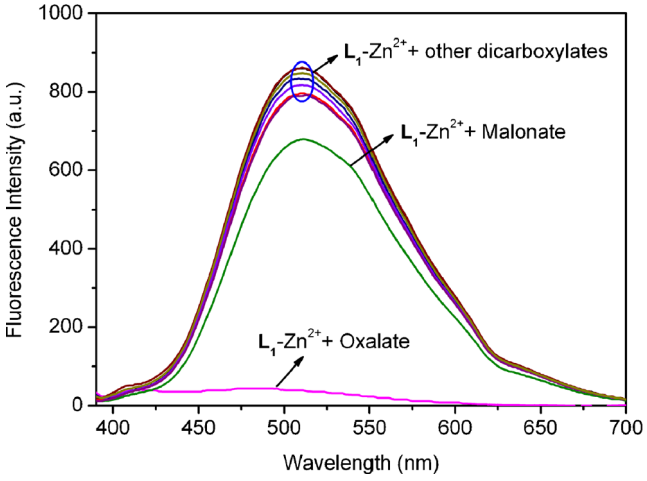

Figure 7. Fluorescence spectra changes of $\mathbf{L_1}$-Zn^{2+}(10 μM) in DMSO-H_2O (1/1, v/v, HEPES 10 mM, pH = 7.4) solution upon addition of 100 equiv. of various dicarboxylates.

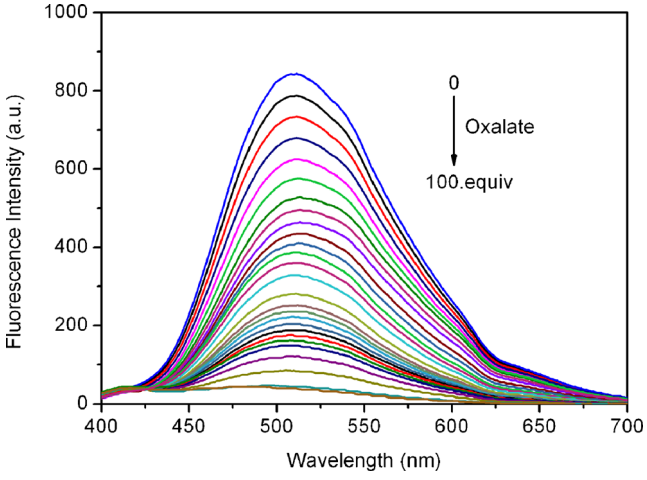

Figure 8. Fluorescence spectra of sensor Zn^{2+}-$\mathbf{L_1}$(10 μM) in DMSO-H_2O (1/1, v/v, HEPES 10 mM, pH = 7.4) solution upon gradual increase in oxalate concentration (0 to 1 mM).

detection limit of the ensemble to oxalate was estimated as 2.06×10^{-5} M (Figure S6). Results of competition experiments reveal that co-existence of equal amount

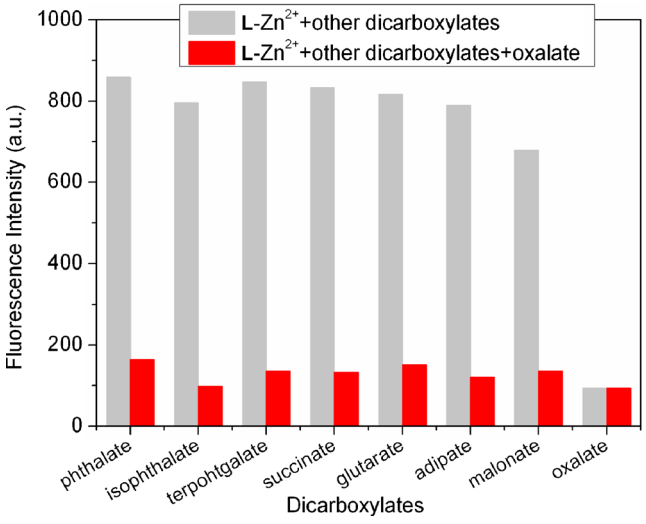

Figure 9. Change in fluorescence intensity of $\mathbf{L_1}$-Zn^{2+} (10 μM) in H_2O-DMSO (1/1, v/v, pH = 7.4) at 512 nm. The gray bars represent the emission intensity of Zn^{2+}-$\mathbf{L_1}$ in the presence of 100 equiv. of competing dicarboxylates; the red bars represent the emission intensity of the above solution upon addition of 100 equiv. of oxalate.

of other dicarboxylates did not cause any remarkable influence on oxalate detection (Figure 9).

3.3 *Living cell imaging studies*

To investigate the practical applicability of $\mathbf{L_1}$ for sequential detection of Zn^{2+} and oxalate, we evaluated its potential utility for imaging Zn^{2+} and oxalate in living cells. The human cervical HeLa cancer cell lines incubated for 0.5 h at 37°C with $\mathbf{L_1}$ (5 μM) showed no fluorescence (Figure 10d). Further addition of Zn^{2+} (10 μM) to the pre-incubated cell for 1h exhibited a noticeable green fluorescence (Figure 10e). However, when oxalate (20 μM) was added to HeLa cell which was incubated with $\mathbf{L_1}$ (10 μM) and Zn^{2+}(10 μM) for 30 min at 37°C, the previous observed green fluorescence was quenched greatly (Figure 10f). These results indicate that $\mathbf{L_1}$ can be used as a sensor to probe the intracellular Zn^{2+} and oxalate.

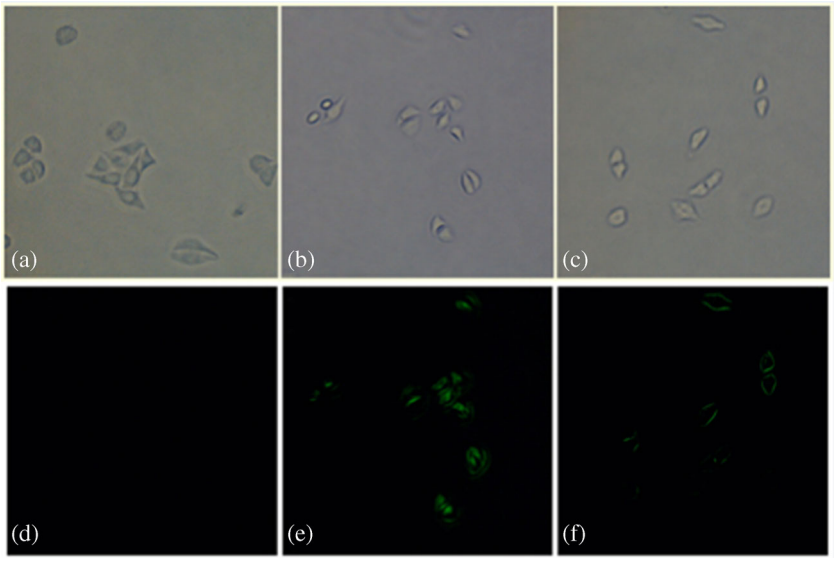

Figure 10. Fluorescence images of Zn^{2+} and oxalate in HeLa cells. (d and a) Fluorescence image of HeLa cells with addition of $\mathbf{L_1}$ and its bright field image. (e and b) Fluorescence image of HeLa cells incubated with $\mathbf{L_1}$(5 μM) for 30 min at 37°C and then incubated with Zn^{2+}(10 μM) for 30 min at 37°C and its bright-field image. (f and c) Fluorescence images of HeLa cell incubated with $\mathbf{L_1}$(10 μM) and Zn^{2+}(10 μM) for 30 min at 37°C and then incubated with oxalate (20 μM) for 30 min at 37°C and its bright field image.

4. Conclusions

In summary, we have developed a new fluorescence sensor based on Schiff base ($\mathbf{L_1}$) for relay recognition of Zn^{2+} and oxalate in aqueous media. Sensor $\mathbf{L_1}$ exhibits high selectivity and sensitivity for sequential detection of Zn^{2+} and oxalate with good anti-inferences ability. Imaging studies of living HeLa cells imaging studies indicate that this new fluorescent sensor holds great potential for biological applications for relay detection of Zn^{2+} and oxalate. Since the *S* enantiomer of binaphthol derivative was used in this work, we anticipate that the *in situ* formed chiral zinc complex could exert recognition behavior to a chiral analyte in a future work.

Supplementary Information

Supplementary Information (Figures S1–S6) is available at www.ias.ac.in/chemsci.

Acknowledgements

We are grateful to the National Natural Science Foundation of China (No. 21176029, 21476029), Liaoning BaiQianWan Talents Program (No. 2012921057), and the Program for Liaoning Excellent Talents in University (LR2015001) for financial support.

References

1. Berg J M and Shi Y 1996 *Science* **271** 1081
2. Walker C F and Black R E 2004 *Annu. Rev. Nutr.* **24** 255
3. (a) Chen Y, Bai Y, Han Z, He W and Guo Z 2015 *Chem. Soc. Rev.* **44** 4517; (b) Jiang P and Guo Z 2004 *Coord. Chem. Rev.* **248** 205; (c) Xu Z, Yoon J and Spring D R 2010 *Chem. Soc. Rev.* **39** 1996; (d) Bhaumik C, Maity D, Das S and Baitalik S 2012 *RSC Adv.* **2** 2581; (e) Mardanya S, Karmakar S, Das S and Baitalik S 2015 *Sens. Actuators, B* **206** 701; (f) Mondal D, Bar M, Maity D and Baitalik S 2015 *J. Phys. Chem. C* **119** 25429; (g) Ding A, Tang F, Wang T, Tao X and Yang J 2015 *J. Chem. Sci.* **127** 375; (h) Chao D 2016 *J. Chem. Sci.* **128** 133
4. Capra R H, Strumia M, Vadgama P M and Baruzzi A M 2005 *Anal. Chimi. Acta* **530** 49
5. Li H, Chai X-S, DeMartini N, Zhan H and Fu S 2008 *J. Chromatogr. A* **1192** 208
6. Liu Y, Huang J, Wang D, Hou H and You T 2010 *Anal. Methods* **2** 855
7. (a) Tang L, Park J, Kim H-J, Kim Y, Kim S J, Chin J and Kim K M 2008 *J. Am. Chem. Soc.* **130** 12606; (b) Hu M and Feng G 2012 *Chem. Commun.* **48** 6951; (c) Wang G, Zhu H, Lin Y, Chen Y and Fu N 2015 *Sens. Actuators, B* **206** 624; (d) He C, Qian X, Xu Y, Yang C, Yin L and Zhu W 2011 *Dalton Trans.* **40** 1034
8. (a) Mummidivarapu V S, Nehra A, Hinge V K and Rao C P 2012 *Org. Lett.* **14** 2968; (b) Yang Y, Yin C, Huo F, Chao J and Zhang Y 2014 *Sens. Actuators, B* **204** 402; (c) Tang L, Zhou P, Huang Z, Zhao J and Cai M 2013

Tetrahedron Lett. **54** 5948; (d) Tang L, Cai M, Zhou P, Zhao J, Zhong K, Hou S and Bian Y 2013 *RSC Adv.* **3** 16802; (e) Peng Y, Dong Y-M, Dong M and Wang Y-W 2012 *J. Org. Chem.* **77** 9072; (f) Tang L, Dai X, Cai M, Zhao J, Zhou P and Huang Z 2014 *Spectrochim. Acta, Part A* **122** 656; (g) Kaur N and Alreja P 2015 *J. Chem. Sci.* **127** 1253

9. Ye F, Zheng Z-J, Deng W-H, Zheng L-S, Deng Y, Xia C-G and Xu L-W 2013 *Chem. - Eur. J.* **8** 2242
10. Zhu J-F, Yuan H, Chan W-H and Lee A W M 2010 *Org. Biomol. Chem.* **8** 3957
11. Shi F, Shen J K, Chen D, Fog K, Thirstrup K, Hentzer M, Karlsson J-J, Menon V, Jones K A, Smith K E and Smith G 2011 *ACS Med. Chem. Lett.* **2** 303
12. Sun Y-Q, Wang P, Liu J, Zhang J and Guo W 2012 *Analyst* **137** 3430
13. Zhang Y, Guo X, Si W, Jia L and Qian X 2008 *Org. Lett.* **10** 473
14. Lin W, Yuan L, Cao Z, Feng Y and Long L 2009 *Chem. - Eur. J.* **15** 5096
15. Lu Q, Hou J, Wang J, Xu B, Zhang J and Yu X 2013 *Chin. J. Chem.* **31** 641